

Activation of persulfate and H₂O₂ by using attapulgite-supported sulfide nanoscale zero-valent iron for degradation of p-nitrophenol: a comparative study

Hui Xu^{a,b,*}, Xuefang Zhao^{a,b}, Minzhang Chen^{a,b}, Yong Chen^{a,b,*}

^aCollege of Petrochemical Technology, Lanzhou University of Technology, Lanzhou 730050, China, Tel.: +86-13639317927; emails: xuhui@lut.edu.cn (H. Xu), yongchen2003@126.com (Y. Chen), 2401809692@qq.com (X. Zhao), 1377380676@qq.com (M. Chen)

^bKey Laboratory of Low Carbon Energy and Chemical Engineering of Gansu Province, Lanzhou 730050, China

Received 16 April 2023; Accepted 13 July 2023

ABSTRACT

Highly reactive oxidizing species such as sulfate and hydroxyl radicals have been widely used in oxidative degradation of various organic pollutants. In this paper, attapulgite supported sulfide modified nanoscale zero-valent iron (APT/S-nZVI) was synthesized and utilized to activate persulfate (Ps) and hydrogen peroxide (H₂O₂) for removal of p-nitrophenol (PNP), respectively. The effects of main factors (such as S/Fe molar ratio, oxidant concentration, initial PNP concentration, pH, temperature and others) on the removal of PNP in different systems were investigated. The results showed that the APT/S-nZVI/H₂O₂ system had stronger removal efficiency and faster reaction rate for PNP than that of the APT/S-nZVI/Ps system under the same fitting conditions, but the APT/S-nZVI/Ps system was efficient over a wide pH range of 3–9, while the efficient pH in the APT/S-nZVI/H₂O₂ system was confined to just 3. Among them, dosage of oxidant, pH value and temperature significantly influenced the PNP removal performance by APT/S-nZVI/H₂O₂, while the influence of the molar ratio of S/Fe and the initial concentration of PNP on the PNP removal performance of APT/S-nZVI/Ps system is more obvious. The factors that affect the PNP removal performance are different in two systems due to the different free radicals generated by Fe²⁺ activated Ps and H₂O₂. The underlying mechanism and degradation products of APT/S-nZVI in activating Ps and H₂O₂ were elucidated through UV-Vis spectra and gas chromatography-mass spectrometry. In addition, the effect of different inorganic ions on the degradation of PNP in the two systems was investigated, and the result showed that the common anions certain inhibitory effect on PNP removal, but the degradation of PNP remained above 97%. The study demonstrated that both APT/S-nZVI/Ps and APT/S-nZVI/H₂O₂ system can efficiently remove PNP, but which system is more suitable for the practical application should be according to the requirements of removal and circumstance conditions.

Keywords: Attapulgite; Nano zero valent iron; Sulfur-modified; p-nitrophenol; Removal

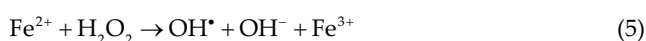
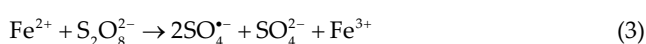
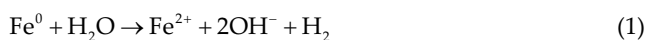
1. Introduction

With the rapid development of industrialization in recent years, a large number of highly toxic pollutants are being discharged freely into the ecosystem, which poses a

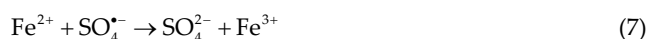
serious threat to the health of humans and wildlife [1]. In particular p-nitrophenol (PNP, C₆H₅NO₃) and its derivatives are extensively used in the manufacture of different kinds of pesticides, pharmaceuticals, and synthetic dyes, which makes it widely used in the chemical industry. However, its

* Corresponding author.

high toxicity, good water solubility and excellent chemical and biological stability make it a potentially toxic pollutant present in natural water and wastewater systems [2] and is also considered one of the most difficultly decomposed persistent organic pollutants [1]. Therefore, it is necessary to develop an efficient treatment approach in order to minimize its bio-refractory and adverse effects on the environment. So as far, there are many methods have been adopted to remove PNP from aquatic environment, such as advanced oxidation process (AOPs) [3], electrochemical technology [4], photocatalysis [5], membrane method [6], adsorption [7], nitration method [8], cross-linked resin [9]. Among these techniques, AOPs as clean and efficient technologies are widely used in the degradation of organic pollutants by free radicals (e.g., hydroxyl radicals, sulfate radicals), which can oxidize most of them into small molecules and even mineralize the intermediates completely. Both of hydroxyl radicals and sulfate radicals possessing strong oxidizing capability may attack PNP, destroy the structure of aromatic ring and obtain a favorable treatment effect through cumulative oxidizability [10,11]. Hydrogen peroxide (H_2O_2) and persulfate (Ps) are the two main precursors for the production of hydroxyl and sulfate radicals and are commonly used in practice [12]. H_2O_2 has strong oxidability under acidic conditions and the produced hydroxyl radical (OH^\bullet) with high potential of 2.7 V. It has attracted much attention for its high degradation efficiency, easy implementation and environmental friendliness to target pollutants. Compared with H_2O_2 , Ps as a more advantageous oxidant have been applied extensively to treat contaminated groundwater and soils due to its solubility and higher chemical stability [13]. It can generate highly oxidative species, sulfate radicals $SO_4^{\bullet-}$ ($E = 2.6$ V) through the activation process and has a longer half-life of 30–40 μ s compared with OH^\bullet . The $SO_4^{\bullet-}$ has an oxidation capacity close to OH^\bullet ($E_0 = 2.7$ V) under acidic conditions, while its oxidation capacity is significantly superior to OH^\bullet under neutral and alkaline conditions [13,14]. Common AOPs usually adopt homogeneous catalysis or heterogeneous catalysis to enhance the yield of OH^\bullet or $SO_4^{\bullet-}$ -oxidizing free radicals [15,16]. In general, nZVI is considered to be a promising heterogeneous catalyst for the reaction. It can gradually release Fe^{2+} , avoiding the rapid depletion and excessive Fe^{2+} induced scavenging reactive oxygen species (ROS) [17]. As a heterogeneous catalysis and substitute of Fe^{2+} , nZVI has strong reactivity and reduction ability ($E_0 = 0.44$ V), and is widely used as an activator for Ps and H_2O_2 to generate active substances [18,19] as expressed by Eqs. (1)–(5).



Although nZVI has been widely used as a catalyst for AOPs, it is easily passivated and agglomerated due to its high surface energy and magnetic properties [20]. The oxidation passivation layer created during the reaction also reduces the reactivity and mobility of the nZVI, resulting in reduced removal of pollutants [21]. The nZVI is similarly susceptible to corrosion and produces large amounts of Fe^{2+} , which may induce the scavenging of $SO_4^{\bullet-}$ and OH^\bullet , as in Eqs. (6) and (7) [14].



To overcome these disadvantages of nZVI and to enhance its practical applications, various strategies have been adopted, such as surface modification, metal doping and loading on the support material [22,23]. In these strategies, sulfation of nZVI has been shown to be very effective in reducing particle aggregation and enhancing the stability of nZVI. Recently studies had demonstrated that sulfide-modified nZVI (S-nZVI) has higher reactivity than that of nZVI and accelerated reductive removal of contaminants, even at high pH [24]. Due to the formation of iron sulphide rather than iron oxide layers on the nZVI surface, S-nZVI has a stronger hydrophobicity and a lower band gap to maintain its reducing power and improve the transfer of electrons [25,26]. In addition, the formation of an iron sulphide layer can effectively slow down the release of Fe^{2+} scavenging radicals by excessive nZVI corrosion. Ps activated with S-nZVI appear to degrade chemical contaminants better than those activated with bare nZVI, suggesting a promising application of S-nZVI/Ps in AOPs processes [27]. The reported researches have shown that S-nZVI can activate Ps and H_2O_2 to generate $SO_4^{\bullet-}$ and OH^\bullet in a similar way to nZVI [Eqs. (1)–(5)] [28–30]. Accordingly, S-nZVI has the potential to be a promising alternative for activating Ps or H_2O_2 for the effective oxidation of organic pollutants.

The select of a suitable substrate for loading nZVI is also an especially significant method, to further improve its dispersion and stabilization. Moreover, supported-nZVI has shown higher stability compared to bare nZVI [31]. The steric stability of nZVI can be enhanced to a certain extent, and the agglomeration can be effectively reduced [32]. As a kind of natural mineral material, attapulgite (APT) has proven to be effective support to improve the stability of nZVI, due to its abundant porous structure, large specific surface area and environmental stability [33]. Moreover, as a green economic adsorbent, it is widely used in the removal of heavy metal ions, dyes and organics [34–36]. In our previous studies, APT-supported sulfidation of nZVI (APT/S-nZVI) was prepared to removal heavy metals. More importantly, due to the porous nature of APT, it can initially disperse and stabilize nanoparticles [37], which could enhance the performance of APT-supported nZVI in environmental applications.

As known, there are many studies about nZVI in activating Ps and H_2O_2 for removal of contaminants [26,38–40]. However, there are very few studies addressing the application of APT/S-nZVI to activate Ps and H_2O_2 for PNP treatment. Besides, the feasibility of S-nZVI in activating other oxidants such as H_2O_2 is yet to be examined. In this study, we have

successfully synthesized APT/S-nZVI and used it to activate Ps and H₂O₂ to oxidative degrade PNP. The feasibility of activating Ps and H₂O₂ for the degradation of PNP in two systems under different conditions was compared and analyzed. The influencing factors (concentration of oxidant, S/Fe mole ratio, initial concentration of PNP, pH, and initial concentrations) are developed, respectively. Moreover, the possible degradation pathways of PNP in different oxidant systems were proposed. We aim to illuminate that the system of APT/S-nZVI coupled with H₂O₂ or Ps as an advanced water treatment method can be a cost-effective and promising strategy for the treatment of the toxic and refractory PNP wastewater.

2. Materials and methods

2.1. Chemical reagents

Attapulgite (APT, 99%) (JC-J503) was purchased from Jiangsu Xuyi Nano-materials Science and Technology Co., Ltd., sodium borohydride (NaBH₄, 98% purity) and potassium persulfate (Ps) were purchased from Shanghai Zhongqin Chemical reagent Co., Ltd. Tert-butanol (TBA) and hydrogen peroxide (H₂O₂, 30%) were purchased from Sinopharm Chemical Reagent Co, Ltd., ferrous sulfate (FeSO₄·7H₂O) was obtained from Yantai Shuangshuang Chemical Co., Ltd., p-nitrophenol (PNP) was supplied by Tianjin Kaixin Chemical Co., Ltd., methanol and dithionite (Na₂S₂O₄) were obtained from Tianjin Fuyu Fine Chemicals Co., Ltd. The solution pH was adjusted using 1.0 M hydrochloric acid (HCl) or sodium hydroxide (NaOH). Sodium bicarbonate (NaHCO₃, 99%), purchased from Tianjin Bodi Chemical Co. Sodium nitrate (NaNO₃, 99%), purchased from Yantai Shuangshuang Chemical Co., Ltd., sodium dihydrogen phosphate (NaH₂PO₄, 99%), purchased from Laiyang Chemical Experimental Factory. All the chemicals were analytical grade and used as received without further purification. Deionized water was used for the preparation of all working solutions within the required concentration.

2.2. Preparation of nZVI and APT/S-nZVI composite

The nZVI and APT/S-nZVI composites were prepared in complete agreement with the preparation steps and methods of our previously published literature [37]. Briefly, 0.045 M NaBH₄ was first mixed with certain amount of Na₂S₂O₄ (0.0015 M, 0.003 M, 0.0045 M and 0.006 M) in 100 mL deionized water, and then added dropwise (about 60 drops·min⁻¹) into 100 mL solution containing 0.018 M FeSO₄·7H₂O and 0.0011 M APT with stirring at 300 rpm to achieve S/Fe molar ratios of 0.1, 0.3, 0.5 and 0.7 in the reaction solution. Afterward, collected blackish particles were washed and cleaned with deionized water and anhydrous ethanol for three times to remove undesirable traces, and dried in a vacuum at 60°C for 7 h. The whole preparation process was executed under nitrogen environment. The preparation method of nZVI is the same as that of S-nZVI, except that Na₂S₂O₄ and APT are not added.

2.3. Batch experiments

0.1 g of APT/S-nZVI was added to 100 mL of PNP solution with a concentration of 50 mg·L⁻¹. The pH of the

solution was adjusted with 1.0 M HCl and NaOH. Before carrying out the adsorption experiment, different amounts of Ps or H₂O₂ were added to the solution and the prepared solution were shaken in a constant-temperature shaker (298 K) at 230 rpm, and the solution was oscillated at a certain temperature. At certain time intervals, 1 mL of the suspension was accurately measured and filtered, and the residual concentration of PNP was measured at λ = 317 nm (pH = 3) using a UV spectrophotometer. In order to study the removal effect of PNP in Ps system and H₂O₂ system, we studied and compared the difference of PNP removal in the two systems under different S/Fe molar ratios (0.1–0.7), oxidant content (0–20 mM), activator different dosage (0.5–2 g·L⁻¹) and pH (3–11). In addition, the effects of temperature (298–318 K) on the removal of PNP in the two systems, as well as the effects of different concentrations (25–100 mg·L⁻¹) on the removal kinetics and thermodynamic parameters of PNP was studied, and the removal rate *R* and adsorption capacity *Q* [Eqs. (8) and (9)] were calculated. The chemical properties of PNP are shown in Table S1.

$$R = \frac{c_0 - c_t}{c_0} \times 100\% \quad (8)$$

$$q = \frac{c_0 - c_t}{m} \times V \quad (9)$$

where *R* (%) represents the removal efficiency of the pollutants; *C*₀ is the initial PNP concentration and *C* denotes the PNP concentration at *t* min; *q* is the adsorption capacity of the dye at *t* min; *V* (L) and *m* (g) are the volume of the adsorbent solution and the mass of the adsorbent, respectively.

2.4. Analysis methods

The concentration of PNP was determined by UV spectrophotometer (UV2355 Lonico Shanghai Instruments Co., Ltd.) and the pH of the solution was detected by (PHS-3D Shanghai Magnetics Instruments Co., Ltd.). The final degradation products of PNP were analyzed by gas chromatography-mass spectrometry (GC 2030 MS QP2020 Japan - Shimadzu), and the chemical properties and crystal structures of S-nZVI before and after the reaction were analyzed by X-ray diffraction (D/MAX-2400X Nihon Rigaku Co.,) and X-ray photoelectron spectroscopy (Zetaszero Nano Malvern Instruments), respectively.

Dissolved ferrous ions (Fe²⁺) were quantified by the 1,10-phenanthroline method [41]. The samples were then analyzed at 510 nm using an ultraviolet-visible spectrophotometer (UV2355 Lonico Shanghai Instruments Co., Ltd.).

3. Results and discussion

3.1. Method optimization

3.1.1. Effects of different materials on the removal of PNP

To demonstrate the superiority of composite material activation Ps and H₂O₂ in the removal of PNP, the removal effects of PNP were studied in different systems at pH = 3.

The results are shown in Fig. 1a and b. From the graph, it can be clearly seen that in the absence of oxidants, the PNP removal rates of APT and nZVI alone were only 9.48% and 45.08%, respectively. Compared with APT and nZVI, the PNP removal efficiency of APT/S-nZVI composite can reach 62.03%. The removal of PNP by nZVI and APT/S-nZVI is mainly due to the reduction of Fe, and the sulfide generated by S-nZVI on the surface of nZVI inhibits its agglomeration to a certain extent [26,42]. Secondly, the introduction of APT makes the dispersion of S-nZVI uniform and increases the active sites, so that APT/S-nZVI has a higher reactivity to PNP and improves the removal efficiency of PNP. When different oxidants are added, APT has no effect on the activation of Ps and H₂O₂. By contrast, the PNP removal efficiency of nZVI and APT/S-nZVI composites is significantly improved, and the removal efficiency is close to 100% in a short period, indicating that free radicals are generated in both Ps and H₂O₂ systems after the addition of oxidants. It can be seen from Fig. 1c and d that the removal rate of PNP by APT/S-nZVI and nZVI are both accelerated after the addition of oxidizer. Compared with Ps system, the removal effect (removal efficiency and reaction rate) is more obvious in H₂O₂ system. The different removal effects in the two systems can be explained by the generation of different types of free radicals. On the one hand, sulfate radical is mainly generated in Ps system, while hydroxyl radical is mainly generated in H₂O₂ system. At pH = 3, the redox potential of SO₄^{•-} ($E = 2.6$ V) is lower than that of OH[•] ($E = 2.7$ V), making the removal effect weak. On the other hand, the SO₄^{•-} generated in the Ps system can form iron complexes with iron species, which cover the surface of the material and have a certain impact on the removal of PNP [14,38]. Therefore,

the follow-up experiments compare the PNP removal effects of the two systems under different conditions to find the best removal conditions under the respective systems. To further highlight the superiority of the S-nZVI material, we investigated the degradation efficiency of the homogeneous Ps/Fe²⁺ and H₂O₂/Fe²⁺ processes parallel to the non-homogeneous activation (S-nZVI activation), as shown in Fig. S1, the removal rates of the H₂O₂ and Ps systems during homogeneous oxidation were 33.10% and 29.03%, respectively, which were much lower than the non-homogeneous S-nZVI system (close to 100%). This is mainly attributed to the fact that Fe²⁺ is rapidly released in large quantities in the homogeneous system and the excess Fe²⁺ can consume some of the free radicals Eqs. (6) and (7) [14], leading to a significant reduction in the removal rate.

3.1.2. Effects of different S/Fe molar ratios on removal of PNP

S/Fe mole ratio plays a key role in the process of APT/S-nZVI activation of Ps and H₂O₂ oxidation removal of PNP. In order to observe the effect of S/Fe mole ratio on PNP removal, APT/S-nZVI composites with S/Fe mole ratio of 0.1, 0.3, 0.5 and 0.7 were studied to activate Ps and H₂O₂ to remove PNP. As shown in Fig. 2a and b, it can be seen that S/Fe molar ratios have slightly different effect on PNP removal in the APT/S-nZVI/Ps and APT/S-nZVI/H₂O₂ systems. Compared with the APT/S-nZVI/H₂O₂ system, APT/S-nZVI/Ps system is more susceptible to S/Fe mole ratio. In the APT/S-nZVI/Ps system, when the S/Fe molar ratio was changed from 0.1 to 0.5, the removal efficiency of PNP did not change much. When the S/Fe molar ratio was 0.3, the removal efficiency was the highest, reaching 99.91%, and time to reach equilibrium

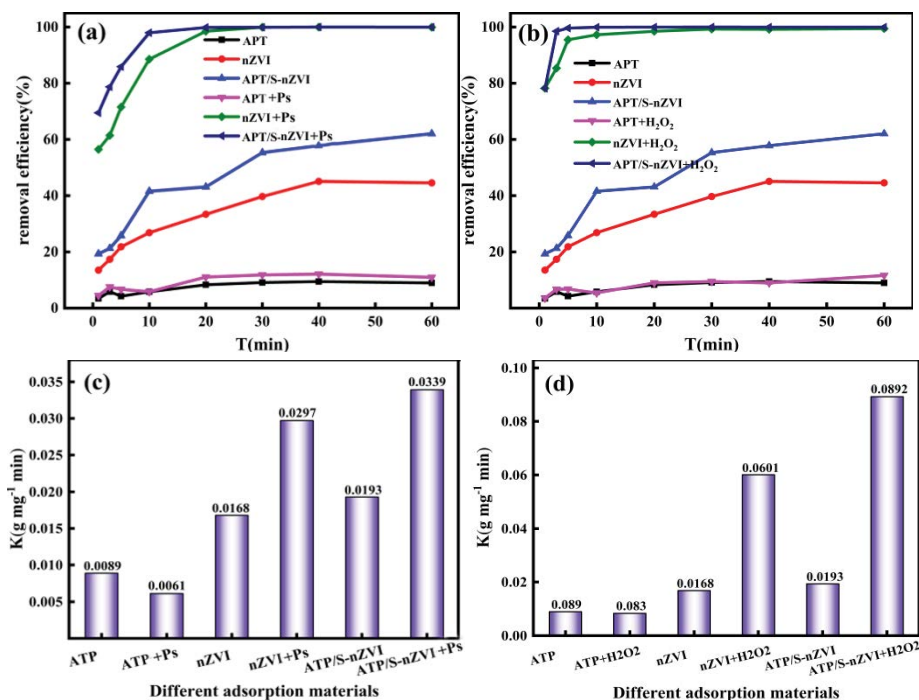


Fig. 1. Effect of different materials on the removal efficiency of PNP and removal rate constant of PNP, respectively. (PNP = 50 mg·L⁻¹, S-nZVI = nZVI = APT = 1 g·L⁻¹, S/Fe = 0.3, initial pH = 3.0, Ps = 6 mM, H₂O₂ = 6 mM).

was the least. While the S/Fe molar ratio was 0.7, the removal efficiency dropped to 98.03%, and the time to reach equilibrium increased. The result indicates that there is an optimal S/Fe molar ratio for the activation of Ps in APT/S-nZVI composites, and the removal efficiency of PNP decreases with the increase of sulfur content. In the APT/S-nZVI/H₂O₂ system, the S/Fe molar ratio in the range of 0.1–0.7 has little effect on the removal efficiency of PNP. When the S/Fe molar ratio is 0.3, the time to reach equilibrium is the shortest.

In order to study the underlying removal mechanism under different S/Fe molar ratios, the changes of Fe and S valence states on the surface of APT/S-nZVI at different S/Fe molar ratios (S/Fe = 0.1, 0.3 and 0.5) were analyzed by X-ray photoelectron spectroscopy (Fig. 2c). Moreover, the X-ray diffraction analysis of as-prepared nZVI and APT/S-nZVI composites can further provide an information of the elements including their oxidation states (Fig. S2). In the spectrum of nZVI, there is a strong and sharp peak at $2\theta = 44.6^\circ$ and no other impurity peaks, which is the characteristic peak of Fe⁰, indicating that the prepared Fe⁰ has high purity and good crystal structure [37]. For APT/S-nZVI, the peaks at $2\theta = 8.6^\circ$, 19.8° and 26.4° correspond to the (110), (040) and (400) planes of APT, respectively [43]. The diffraction peak at $2\theta = 44.6^\circ$ is significantly stronger and sharper than that of nZVI. In addition, a new peak detected at $2\theta = 64.7^\circ$ can be attributed to FeS, which was formed by the modification of sulphur during the synthesis process [44]. As shown in Fig. 2c, the peaks at 710.7 and 724.3 eV should be attributed to Fe(II)-O/Fe(II)-S, which may be present as iron oxides and sulphides. The peaks appearing at 712.6 and 725.8 eV are assigned to Fe(III)-O

[37]. From Fig. 2c, it can be observed that when the S/Fe molar ratio is 0.1, a strong Fe⁰ peak is detected at 706.7 eV, and as the S/Fe molar ratio increases from 0.1 to 0.5, the surface Fe⁰ content gradually decreases. It indicates that with the increase of sulfur content, a large amount of iron sulfide is generated on the surface, which covers the surface of Fe⁰ and makes the peak intensity of Fe⁰ very low. Moreover, the content of surface FeS gradually decreased, which may be due to the change of surface iron sulfide with the increase of sulfur content [38]. It can be observed from spectrum of S2p of Fig. 2d that when the S/Fe molar ratio is 0.1, the FeS content is 43.25%, and when the S/Fe molar ratio increases from 0.1 to 0.5, the surface FeS content decreases to 26.99%, and the FeS_x content from 11.42% increased to 37.67%. While the removal efficiency decreased with the increase of S/Fe molar ratio, possibly related to the abundant FeS_x on the surface. According to previous studies [26], the activity of FeS_x is significantly lower than that of FeS, and with the increase of sulfur content, excess FeS_x covers the surface of Fe⁰, which will block the active sites and reduce the reaction activity. This is also the reason why the removal efficiency decreases with the increase of S/Fe molar ratio. The SO₄²⁻ generated in the APT/S-nZVI/Ps system will form iron complexes and deposit on the surface of the material, resulting in a decrease in the reactivity of APT/S-nZVI [14]. In the APT/S-nZVI/H₂O₂ system, although Fe–O and Fe–S compounds are deposited on the surface of the particles, these iron compounds are still able to activate H₂O₂ to form OH[•] [26]. Therefore, the removal of PNP in the APT/S-nZVI/H₂O₂ system is less affected by the S/Fe molar ratio.

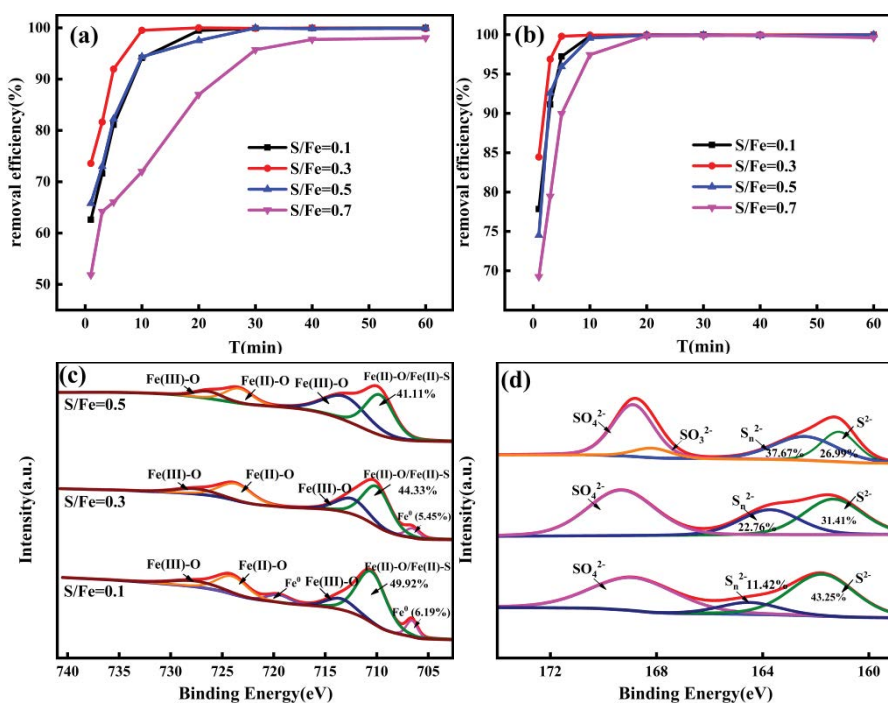
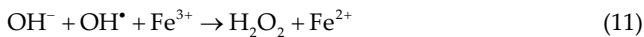


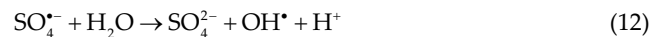
Fig. 2. Effect of different S/Fe molar ratios activated Ps (a) and H₂O₂ (b) on the removal of PNP; X-ray photoelectron spectroscopy survey spectra of different S/Fe molar ratios, (c) Fe2p, (d) S2p; (PNP = 50 mg·L⁻¹, S-nZVI = 1 g·L⁻¹, initial pH = 3.0, Ps = 6 mM, H₂O₂ = 6 mM).

3.1.3. Effects of different pH on removal of PNP

In practical applications, solution pH is an important factor affecting PNP removal. Fig. 3 shows the PNP removal experiments in the pH 3–11 range of the APT/S-nZVI/Ps and APT/S-nZVI/H₂O₂ systems. For the APT/S-nZVI/Ps systems, as can be seen in Fig. 3a, the highest removal efficiency (99.97%) was achieved at pH = 3, with the shortest time to equilibrium. When the pH increased from 3 to 9, the removal efficiency decreased slightly and the time to reach equilibrium became longer, but the final PNP removal efficiency all reached more than 99%. When pH = 11, the removal efficiency dropped to 94.70%. The main reason is that under acidic conditions, due to the rapid corrosion of Fe⁰, a large amount of Fe²⁺ is released to activate Ps and H₂O₂, generating enough SO₄^{•-} and OH[•] radicals, which accelerates the oxidation reaction and is more effective for the removal of PNP. Under alkaline conditions, the activity of Fe⁰ is weakened by surface passivation [38,39]. The removal of PNP in the APT/S-nZVI/H₂O₂ system was greatly affected by pH (Fig. 3b), indicating that the APT/S-nZVI/H₂O₂ system was more susceptible to pH, mainly because the redox potential of OH[•] was affected by pH greater impact. With the increase of pH, the redox potential of OH[•] decreased and the attack ability to PNP molecules is weakened. In addition, when pH > 5, H₂O₂ will rapidly self-decompose, resulting in less OH[•] being generated and thus affecting the removal of PNP [Eqs. (10) and (11)] [40,45].



The effect of solution pH on the removal of PNP from the APT/S-nZVI/Ps system can also be illustrated by the change in solution pH during the experiment. Fig. 3c is the change of pH value of the solution in the APT/S-nZVI/Ps system. Before the reaction, the pH of the solution was in the range of 3–9, and dropped rapidly to about 3–4 after the reaction 10 min. However, in APT/S-nZVI/H₂O₂ system (Fig. 3d), the pH of the solution did not change significantly after the reaction, which may be the reason why the two systems have different PNP removal performance at different pH. In the APT/S-nZVI/Ps system, the pH of the initial solution was 3–9, and the pH dropped significantly after the reaction, indicating that a large amount of H⁺ was generated during the reaction, which may be related to the rapid reaction of Fe⁰ and Ps [Eqs. (4) and (12)]. The no passivation occurs on the Fe⁰ surface, thus not affecting the removal efficiency of PNP [38]. When the pH of the initial solution was 11 and the reaction is neutral or weak alkaline medium, the passivation of the Fe⁰ surface will have a certain influence on PNP. In the APT/S-nZVI/H₂O₂ system, the pH did not change much during the experiment, indicating that with the change of pH, the surface passivation of Fe⁰ reduces the removal efficiency of PNP, which is also the reason why APT/S-nZVI/H₂O₂ is more susceptible to pH affect.



3.1.4. Variation of Fe²⁺ concentration at different pH values

Since Fe²⁺ is a key species for the activation of oxidants to generate free radicals for the degradation of PNP, the

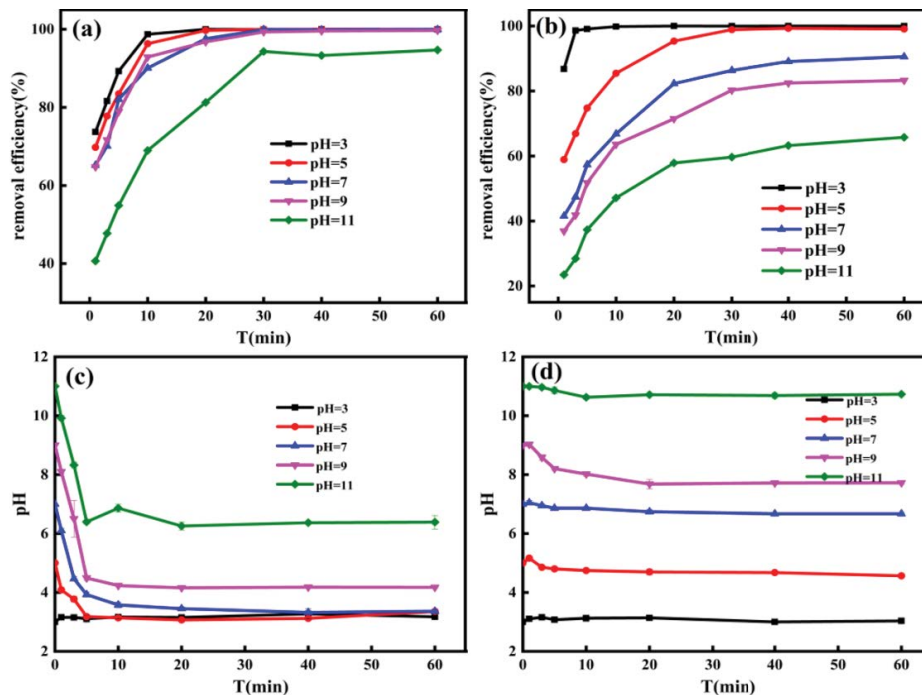


Fig. 3. Effect of initial pH on PNP removal in (a) APT/S-nZVI/Ps system and (b) APT/S-nZVI/H₂O₂ system; the variation of solution pH during the reaction process in (c) APT/S-nZVI/Ps system and (d) APT/S-nZVI/H₂O₂ system (PNP = 50 mg·L⁻¹, S-nZVI = 1 g·L⁻¹, S/Fe = 0.3, Ps = 6 mM, H₂O₂ = 6 mM).

difference in the degradation rate of PNP at different pH may be due to the difference in Fe^{2+} concentration, so we investigated the leaching concentration of Fe^{2+} at different pH values (pH = 3, 7 and 9) using the 1,10-phenanthroline method [41], as shown in Fig. 4a and b. It can be seen from the figures that the leaching rates of Fe^{2+} in the Ps and H_2O_2 systems were essentially the same at pH = 3, but at pH = 7 and 9, the concentration of Fe^{2+} in the Ps system was significantly higher than that in the H_2O_2 system. This is mainly because, at pH = 3, the pH of the Ps and H_2O_2 systems remained essentially unchanged at around 3 during the reaction (shown in Fig. 3c and d), and therefore the concentrations of Fe^{2+} produced by corroding S-nZVI under acidic conditions were almost similar. However, at pH values of 7 and 9, the solution in the Ps system gradually became more acidic during the reaction (shown in Fig. 3c), while the pH in the H_2O_2 system remained almost constant (shown in Fig. 3d), which resulted in the S-nZVI surface being passivated and therefore producing a lower concentration of Fe^{2+} .

3.1.5. Effect of oxidant addition on the removal of PNP

Different oxidants activated by APT/S-nZVI composites have different degrees of PNP removal efficiency, and the concentration of oxidant also plays a key role in the removal of PNP. The effect of Ps concentration is shown in Fig. 5a. When the concentration of Ps was increased from 0 to 20 mM,

the removal efficiency increased from 62.03% to 99.98%. It shows that the increase of Ps concentration is beneficial to the removal of PNP. Although excess Ps also produces a certain scavenging of free radicals [46,47], the scavenging effect is not obvious in this concentration range (0–20 mM). Compared with the APT/S-nZVI/Ps system, the APT/S-nZVI/ H_2O_2 system showed different removal trends of PNP with the change of H_2O_2 concentration. As shown in Fig. 5b, with the increase of H_2O_2 concentration from 0 to 6 mM, the removal efficiency of PNP increased from 62.03% to 99.99%. It indicated that within the appropriate range of H_2O_2 concentration, with the increase of H_2O_2 concentration, more OH^{\bullet} is generated, which improves the removal efficiency of PNP. However, with the increase of H_2O_2 concentration from 6 to 20 mM, the removal efficiency decreases from 99.99% to 92.79%. This is because excessive H_2O_2 will cause useless consumption of OH^{\bullet} , resulting in the removal of OH^{\bullet} [39]. Therefore, the dosage of H_2O_2 should be carefully optimized in practical applications to ensure the removal efficiency.

3.1.6. Effects of different initial concentrations on the removal of PNP

The effect of different initial concentrations (25–100 $\text{mg}\cdot\text{L}^{-1}$) of PNP on the removal of PNP (pH = 3) under the APT/S-nZVI/Ps and APT/S-nZVI/ H_2O_2 systems was investigated as shown in Fig. 6. With the increase of initial concentration of

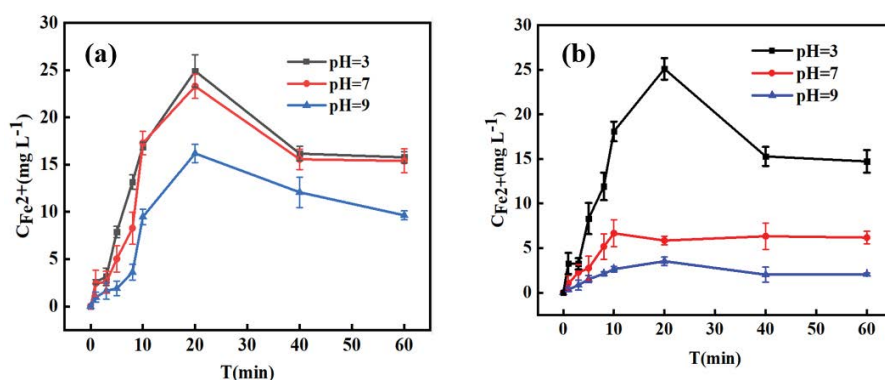


Fig. 4. Variation of Fe^{2+} concentration in Ps (a) and H_2O_2 (b) systems at different pH values (PNP = 50 $\text{mg}\cdot\text{L}^{-1}$, S-nZVI = 1 $\text{g}\cdot\text{L}^{-1}$, S/Fe = 0.3, Ps = 6 mM, H_2O_2 = 6 mM, (initial concentration of Fe^{2+} is 1 mM)).

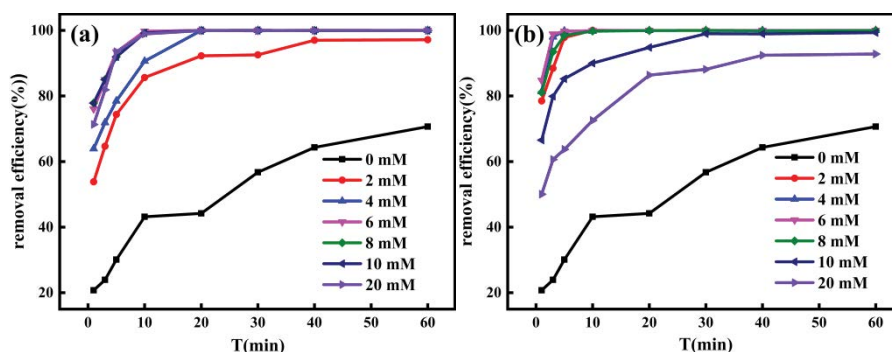


Fig. 5. Effect of different oxidants dosage on the removal of PNP in (a) APT/S-nZVI/Ps system and (b) APT/S-nZVI/ H_2O_2 system (PNP = 50 $\text{mg}\cdot\text{L}^{-1}$, S-nZVI = 1 $\text{g}\cdot\text{L}^{-1}$, S/Fe = 0.3, initial pH = 3.0).

PNP, the removal efficiency of PNP in APT/S-nZVI/Ps and APT/S-nZVI/H₂O₂ systems displayed same trends. As shown in Fig. 6a, in APT/S-nZVI/Ps system, when the initial concentration of PNP increases from 25 to 100 mg·L⁻¹, the maximum removal efficiency of PNP decreases from 99.99% to 94.53%, the equilibration time increases and the removal efficiency decreases. In contrast, the initial concentration of PNP had little effect on the removal efficiency of PNP in the APT/S-nZVI/H₂O₂ system (Fig. 6b). Even if the initial concentration of PNP was increased from 25 to 100 mg·L⁻¹, the removal efficiency be maintained above 99%. From the instantaneous rate (Fig. 6c), it can be found that the instantaneous rate of PNP degradation in the APT/S-nZVI/H₂O₂ system is significantly higher than that in the APT/S-nZVI/Ps system under different initial concentrations. The reason for the difference may be due to the different radicals produced in different systems, which have different oxidative abilities for PNP removal. As previously discussed, the redox potential of OH· is higher than that of SO₄^{·-} at pH = 3. Therefore, the APT/S-nZVI/H₂O₂ system has a superior oxidation capacity than the APT/S-nZVI/Ps system [48].

3.1.7. Effect of temperature on the removal of PNP

As depicted in Fig. 7, the influence of temperature on PNP degradation of APT/S-nZVI/Ps and APT/S-nZVI/H₂O₂ systems. The PNP removal experiments were carried out at different temperatures (298–308 K). In the APT/S-nZVI/Ps system (Fig. 7a), when the temperature increased from 298 to 308 K, the removal efficiency of PNP did not change

significantly, but the equilibrium time was significantly shortened and the removal efficiency of PNP was improved. The reason for the improved removal efficiency of PNP is related to the generation of additional SO₄^{·-} by Ps through heating [49,50]. Higher temperature has a positive effect on the activation of Ps and the degradation of pollutants. At lower temperature, the Ps releases SO₄^{·-} radical slowly, but it can be maintained for a long time. However, at higher temperatures, more SO₄^{·-} can be formed in a shorter time, which is conducive to the degradation of PNP and improve the degradation efficiency, and this process will consume the catalyst faster [50]. The opposite results were observed in the APT/S-nZVI/H₂O₂ system (Fig. 7b). As the temperature increased from 298 to 308 K, the removal efficiency of PNP decreased from 99.99% to 72.93%. The removal efficiency of PNP was significantly higher at 298 and 308 K than at other temperatures, mainly because higher temperature would promote the decomposition of H₂O₂ into O₂ and H₂O instead of generating OH· radicals [45,51]. This is also the reason why the effect of temperature on the removal efficiency of PNP in the two systems is significantly different.

3.1.8. Effect of radical terminator on the removal of PNP

Considering that the removal of PNP is including APT/S-nZVI activation of Ps and H₂O₂ to generate OH· and SO₄^{·-} radicals for oxidation, it is necessary to determine the main active substances for PNP oxidation degradation in APT/S-nZVI/Ps and APT/S-nZVI/H₂O₂ systems. Free radical scavenger methanol and tert-butanol were used to analyze the

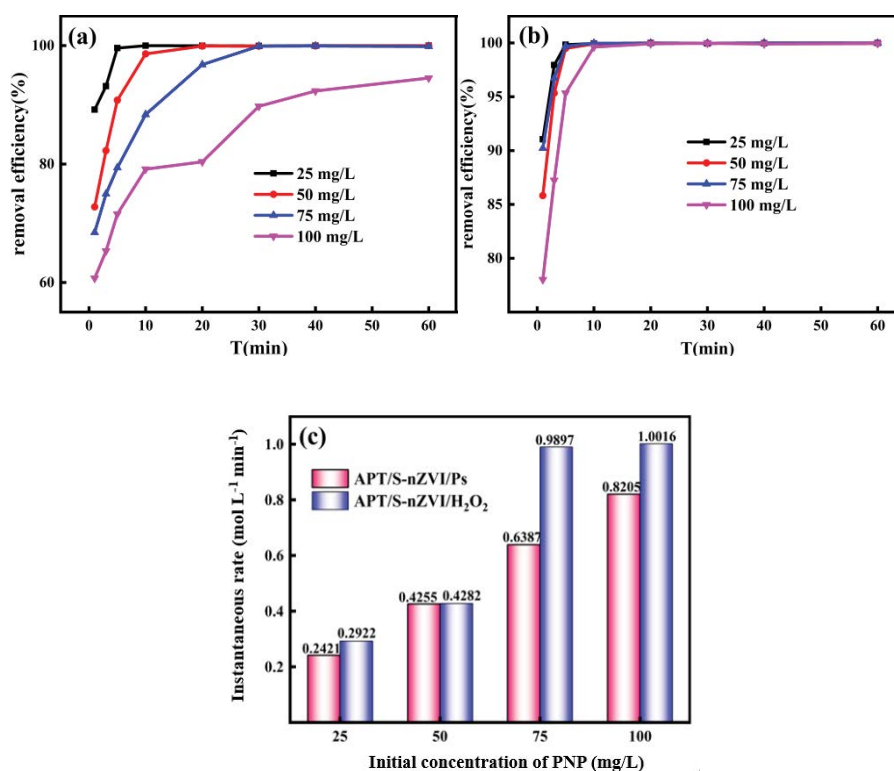


Fig. 6. Effect of different initial concentrations on PNP removal in (a) APT/S-nZVI/Ps system and (b) APT/S-nZVI/H₂O₂ system; (c) instantaneous rates of PNP degradation in different systems (S-nZVI = 1 g·L⁻¹, S/Fe = 0.3, initial pH = 3.0, Ps = 6 mM, H₂O₂ = 6 mM).

main roles of oxides responsible for degradation of PNP in different systems. The reaction rates of methanol with OH^\bullet and $\text{SO}_4^{\bullet-}$ are 9.7×10^8 and $2.5 \times 10^7 \text{ mol}^{-1}\cdot\text{s}^{-1}$, respectively, while the reaction rates of tert-butanol with hydroxyl radicals ($(3.8\text{--}7.6) \times 10^8 \text{ mol}^{-1}\cdot\text{s}^{-1}$) is much higher than the reaction rate with sulfate radicals ($(4.0\text{--}9.1) \times 10^5 \text{ mol}^{-1}\cdot\text{s}^{-1}$) [13,52]. Therefore, methanol acts as a scavenger for OH^\bullet and $\text{SO}_4^{\bullet-}$, while tert-butanol mainly acts as a scavenger for OH^\bullet . The effects of free radical scavengers on the degradation of PNP under different systems are shown in Fig. 8. The comparison between Fig. 8a and b shows that in APT/S-nZVI/Ps systems, the dosage of methanol and tert-butanol increases from 0 to 100 mM, respectively, and the removal efficiency of PNP decreases from 99.99% to 68.93% and 95.91%, respectively. It

can be seen that both free radicals are involved in the degradation of PNP, and $\text{SO}_4^{\bullet-}$ is the main active species. Tert-butanol has little effect on PNP because the reaction of $\text{SO}_4^{\bullet-}$ and PNP is sufficient to compete with that of tert-butanol and $\text{SO}_4^{\bullet-}$. Therefore, the capture of free radicals by tert-butanol can inhibit the reaction rate to a certain extent, but it has little effect on the degradation of PNP. However, previous studies showed that in the APT/S-nZVI/ H_2O_2 system, OH^\bullet was the main active species. It can be seen from Fig. 8c and d that the addition of methanol and tert-butanol significantly decreased the removal efficiency of PNP. Therefore, $\text{SO}_4^{\bullet-}$ plays a major role in the removal of PNP in APT/S-nZVI/Ps system, while OH^\bullet is mainly responsible for the removal of PNP in APT/S-nZVI/ H_2O_2 system.

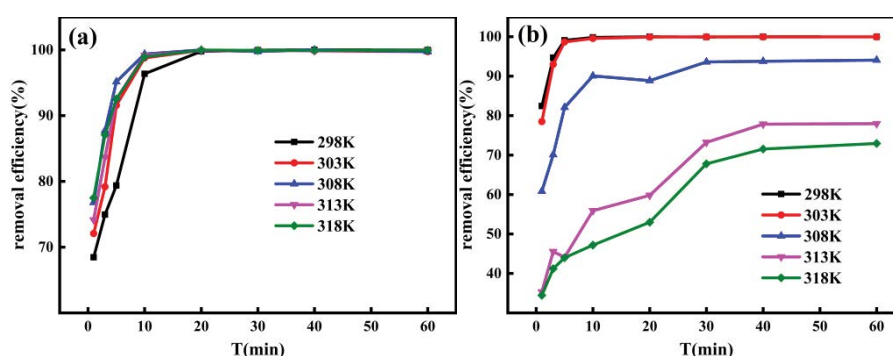


Fig. 7. Effect of temperature on the removal of PNP in (a) APT/S-nZVI/Ps system and (b) APT/S-nZVI/ H_2O_2 system (PNP = $50 \text{ mg}\cdot\text{L}^{-1}$, S-nZVI = $1 \text{ g}\cdot\text{L}^{-1}$, S/Fe = 0.3, initial pH = 3.0, Ps = 6 mM, H_2O_2 = 6 mM).

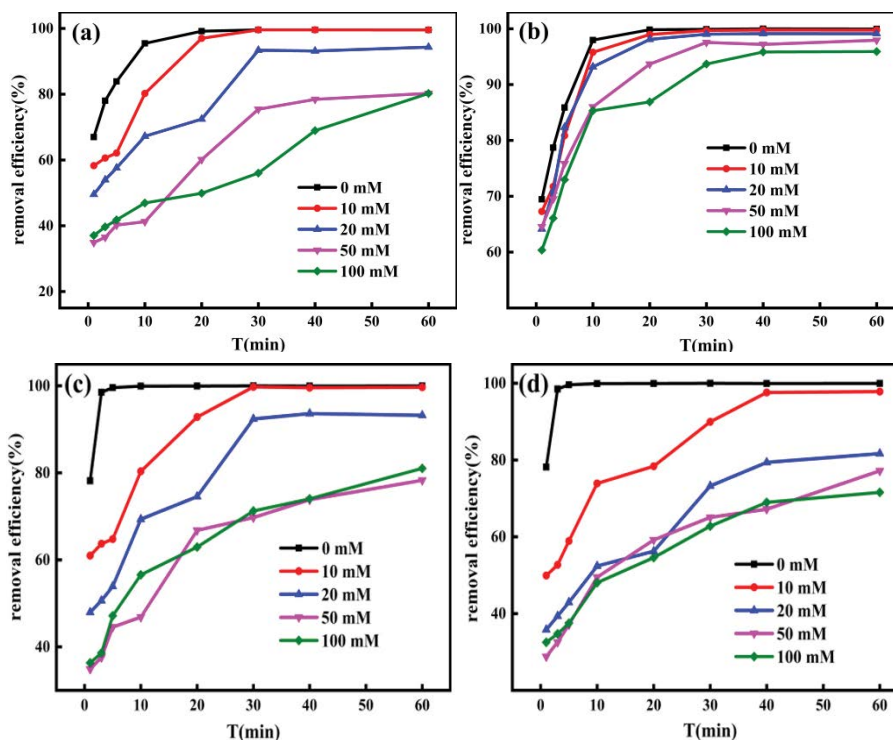


Fig. 8. Effect of radical terminator on removal of PNP (Ps: (a) methanol, (b) tert-butanol and H_2O_2 ; (c) methanol, (d) tert-butanol) (PNP = $50 \text{ mg}\cdot\text{L}^{-1}$, S-nZVI = $1 \text{ g}\cdot\text{L}^{-1}$, S/Fe = 0.3, initial pH = 3.0, Ps = 6 mM, H_2O_2 = 6 mM).

3.1.9. Effect of water matrices

The presence of inorganic anions in the actual wastewater usually has an impact on the removal of the target pollutant. The HCO_3^- , NO_3^- and H_2PO_4^- anions, which considered as most common water matrices were selected as probe ions [53,54]. As shown in Fig. 9, the presence of all these inorganic anions has a certain inhibitory effect on the removal of PNP, but the degradation of PNP remained above 97%. Among these anions, HCO_3^- having the greatest effect on both systems and a greater effect on H_2O_2 systems than on Ps systems. This is attributed to that HCO_3^- can quench reactive radicals, resulting in weaker reactive free radicals [55]. Moreover, the presence of HCO_3^- could increase the pH of the solution to prevent the corrosion of Fe^0 and the generation of SO_4^{2-} [54]. The presence of NO_3^- also has an inhibitory effect on the removal of PNP, mainly because of the passivation of NO_3^- on the surface of S-nZVI, resulting in S-nZVI core Fe^0 is difficult to release [56]. Besides, the weak inhibitory effect of NO_3^- might be attributed to that NO_3^- competed with Ps and H_2O_2 for electrons on the Fe^0 surface and converted to ammonium [55], reducing the reaction with Ps and H_2O_2 . The H_2PO_4^- has a similar mechanism of action to HCO_3^- as

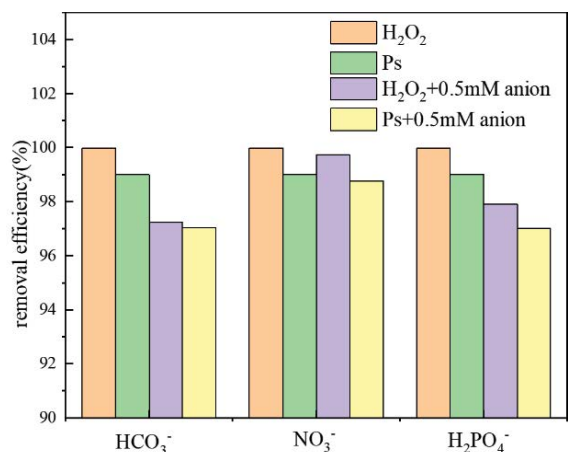


Fig. 9. Effect of different anions (HCO_3^- , NO_3^- and H_2PO_4^-) on the degradation of PNP (PNP = $50 \text{ mg}\cdot\text{L}^{-1}$, S-nZVI = $1 \text{ g}\cdot\text{L}^{-1}$, S/Fe = 0.3, initial pH = 3.0, Ps = 6 mM, H_2O_2 = 6 mM, $\text{HCO}_3^- = \text{NO}_3^- = \text{H}_2\text{PO}_4^- = 0.5 \text{ mM}$).

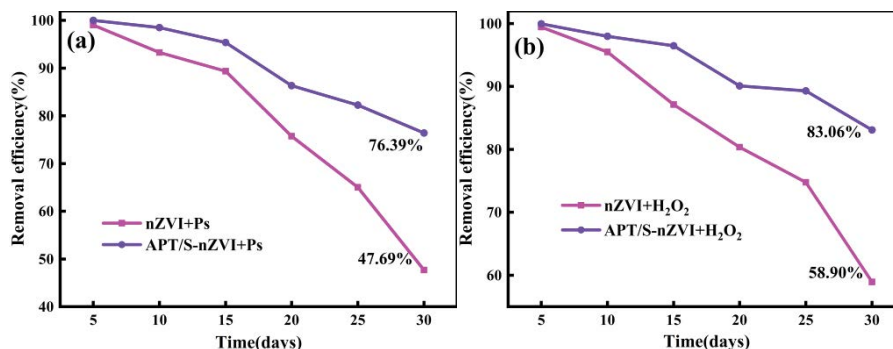


Fig. 10. Effect of placement time on degradation of PNP by APT/S-nZVI in Ps and H_2O_2 systems (PNP = $50 \text{ mg}\cdot\text{L}^{-1}$, S-nZVI = $1 \text{ g}\cdot\text{L}^{-1}$, S/Fe = 0.3, initial pH = 3.0, Ps = 6 mM, H_2O_2 = 6 mM).

a free radical quencher, and also has a certain inhibitory effect on PNP removal [54].

3.2. Stability of APT/S-nZVI and nZVI in two systems

Generally, pristine nZVI features a lack of stability, limiting its applications in groundwater decontamination [57]. In previous studies [37,58], it has been confirmed that the oxidation resistance of nZVI can be improved by vulcanization modification. In addition, S-nZVI on the support can improve colloidal stability in suspension and provide better control of aggregate size [59]. In order to investigate the stability of the APT/S-nZVI on the removal of PNP, under the same external conditions, the nZVI and APT/S-nZVI composites were placed in air for different times, and the removal of PNP by the activated Ps (Fig. 10a) and H_2O_2 (Fig. 10b) were compared. As can be seen from Fig. 9, the oxidation resistance and stability of APT/S-nZVI is significantly improved compared to pure nZVI. The removal efficiencies of PNP by the APT/S-nZVI activated Ps and H_2O_2 systems were 76.39% and 83.06%, respectively, which were much higher than the removal efficiencies of nZVI under the same storage time. It shows that vulcanization and introduction of APT has a good protective effect on nZVI and greatly improves the long-term stability of nZVI.

3.3. Degradation mechanism of PNP in Ps and H_2O_2 system

To investigate the degradation mechanism of PNP under the two systems, the degradation products of PNP were analyzed by UV-Vis spectroscopy at different times. Fig. 11a shows the UV-Vis spectra of PNP degraded in the APT/S-nZVI/Ps system. The absorbance at 317 nm is caused by the conjugation of the benzene ring and the chromophore $-\text{NO}_2$. Both the benzene ring and $-\text{NO}_2$ contain π -bonded electrons, which are prone to π - π^* transitions, thereby shifting the absorption peak to long wavelengths [60]. With the degradation reaction proceeded, the absorbance intensity at 317 nm decreased significantly and disappeared in about 10 min, which proved that PNP could be effectively degraded under the APT/S-nZVI/Ps system. The gradual appearance of a new peak at 296 nm is due to the combined action of the benzene ring and $-\text{NH}_2$, which corresponds to p-aminophenol. It indicated that PNP is mainly reduced to p-aminophenol at first step by H^\bullet and Fe^{2+} that may be produced in the system

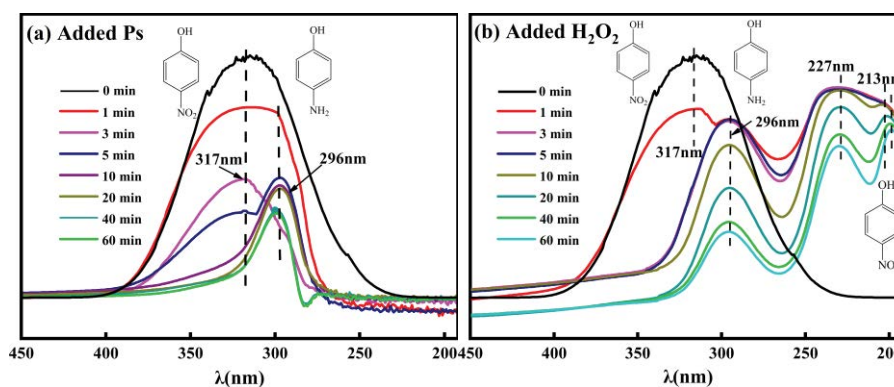
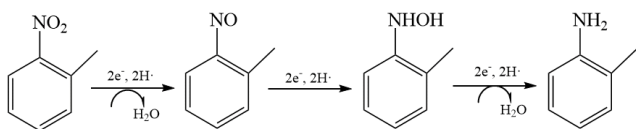


Fig. 11. UV-Vis spectra of degradation of PNP by APT/S-nZVI in Ps and H₂O₂ systems.

under acidic conditions, which can significantly reduce the toxicity of PNP wastewater. Reduction of $-\text{NO}_2$ to $-\text{NH}_2$ is also the main reaction of zero-valent iron reduction and degradation of nitro compounds [Eq. (22)] [48,61]. With the increasing the reaction time, $\text{SO}_4^{\cdot-}$ begins to play a role in the oxidative degradation during PNP removal. The p-aminophenol or PNP is degraded by $\text{SO}_4^{\cdot-}$ oxidation. However, it is not obvious in the UV-Vis spectroscopy, mainly because the products form organic compounds with higher molecular weight through complexation, which can be verified by gas chromatography-mass spectrometry (GC-MS).



The UV-Vis spectra of removal PNP solution in the APT/S-nZVI/H₂O₂ system is shown in Fig. 11b. The absorption peak at 317 nm disappeared within 3 min, proving that the degradation efficiency of PNP in APT/S-nZVI/H₂O₂ system is more efficient than that in APT/S-nZVI/Ps system. The peak at around 208 nm is considered to be the E_2 absorption band of a single benzene ring, and the absorption peak shifts to the long-wave direction, possibly substituted by groups such as $-\text{OH}$. The new peak at 213 nm is thought to be p-nitrosophenol. The absorption peak at 227 nm is caused by the $p-p^*$ transition in the benzene ring of the mono-aromatic hydrocarbon, and part of the PNP is degraded by opening the benzene ring [48]. In the APT/S-nZVI/Ps system, PNP is difficult to be degraded by the ring-opening reaction, which also indicates that OH^{\cdot} has higher energy and activity than $\text{SO}_4^{\cdot-}$ at pH = 3.

To further investigate the degradation products, we used GC-MS to analyze the intermediate products of PNP degradation. In APT/S-nZVI/Ps system, the intermediates obtained by degradation are shown in Table S2, mainly including p-aminophenol (26.692 min), ammonia (9.594–11.919 min) and other degradation products (complexation between intermediate) or impurities (4.972 and 15.095 min). The PNP is degraded small molecules (Mainly including PAP and HQ) by $\text{SO}_4^{\cdot-}$ oxidation, and the products form organic compounds with larger molecular weight through complexation.

The results indicated that $\text{SO}_4^{\cdot-}$ played a role in the oxidative degradation during PNP removal.

The main degradation products obtained in APT/S-nZVI/H₂O₂ system are shown in Table S3, including p-aminophenol (26.699 min), p-benzoquinone (14.745 min), ammonia (8.999 min), small molecules (12.598 min glycolic acid, ketene, etc.) and others unknown compounds (complexation between intermediate). The above results indicated that the main degradation products of PNP in the APT/S-nZVI/Ps system were p-aminophenol, while the main products in the APT/S-nZVI/H₂O₂ system were the mixtures of p-aminophenol, p-benzoquinone and small molecules. In summary, the main possible degradation pathways of PNP in the two systems under acidic conditions are proposed as shown in Fig. S4. The results indicated that the PNP degradation process mainly consist of reduction and oxidation reactions, but the degree of the two types is different for two systems. In the APT/S-nZVI/H₂O₂ system, while PNP is reduced to p-aminophenol, or oxidized to p-benzoquinone, the degradation products are feasibility to undergo ring-opening reactions to form small molecule compounds due to the OH^{\cdot} with high redox potential at pH = 3. In the APT/S-nZVI/Ps system, it is difficult to further degrade PNP and some other reaction products through the ring-opening reaction. By comparison, APT/S-nZVI activated H₂O₂ degradation of PNP is considered to be more effective pretreatment methods due to the less toxic than its parent compound.

4. Conclusions

In this study, the APT/S-nZVI/Ps and APT/S-nZVI/H₂O₂ systems showed good removal of PNP, with the APT/S-nZVI/H₂O₂ system having a stronger removal capacity at pH = 3. The APT/S-nZVI/Ps system was more susceptible to the influence of the S/Fe molar ratio. However, the effects of oxidant dosage, temperature and pH on the removal of PNP were more pronounced for the APT/S-nZVI/H₂O₂ system. The pH range for the APT/S-nZVI/Ps system was wider, whereas in the APT/S-nZVI/H₂O₂ system it was only suitable for acidic environments. It was found that the inorganic ions HCO_3^- , NO_3^- and H_2PO_4^- of common water bodies inhibited the removal of PNP in both systems, but the removal rate was still above 97%, indicating the suitability of the material.

In addition, it was found that the main degradation product of PNP in the APT/S-nZVI/Ps system was p-aminophenol, while the products in the APT/S-nZVI/H₂O₂ system included many small molecules. These findings suggest that the system of S-nZVI/APT coupled with H₂O₂ and Ps could be a promising strategy for the pretreatment of toxic and difficult wastewater.

Acknowledgment

This work was supported by the National Natural Science Foundation of China (NSFC) (52163025, 51503092 and 51763015) the Program for Hongliu First-class Discipline Construction in Lanzhou University of Technology.

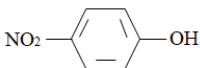
References

- [1] Y. Lu, Y. Xu, Q. Wu, H. Yu, Y. Zhao, J. Qu, M. Huo, X. Yuan, Synthesis of Cu₂O nanocrystals/TiO₂ photonic crystal composite for efficient p-nitrophenol removal, *Colloids Surf., A*, 539 (2018) 291–300.
- [2] J.A. Herrera-Melián, A.J. Martín-Rodríguez, A. Ortega-Méndez, J. Araña, J.M. Doña-Rodríguez, J. Pérez-Peña, Degradation and detoxification of 4-nitrophenol by advanced oxidation technologies and bench-scale constructed wetlands, *J. Environ. Manage.*, 105 (2012) 53–60.
- [3] O. Gimeno, M. Carbajo, F.J. Beltrán, F.J. Rivas, Phenol and substituted phenols AOPs remediation, *J. Hazard. Mater.*, 119 (2005) 99–108.
- [4] X. Wu, X. Song, H. Chen, J. Yu, Experimental study and quantum chemical calculation of free radical reactions in p-nitrophenol degradation during electrochemical oxidation process, *J. Water Process Eng.*, 40 (2021) 101769, doi: 10.1016/j.jwpe.2020.101769.
- [5] S.A. Younis, E. Amdeha, R.A. El-Salamony, Enhanced removal of p-nitrophenol by β-Ga₂O₃-TiO₂ photocatalyst immobilized onto rice straw-based SiO₂ via factorial optimization of the synergy between adsorption and photocatalysis, *J. Environ. Chem. Eng.*, 9 (2021) 104619, doi: 10.1016/j.jece.2020.104619.
- [6] X. Zhu, Z. Pan, H. Jiang, Y. Du, R. Chen, Hierarchical Pd/Uio-66-NH₂-SiO₂ nanofibrous catalytic membrane for highly efficient removal of p-nitrophenol, *Sep. Purif. Technol.*, 279 (2021) 119731, doi: 10.1016/j.seppur.2021.119731.
- [7] Y. Yue, Y. Wang, C. Qu, X. Xu, Modification of polyacrylonitrile-based activated carbon fibers and their p-nitrophenol adsorption and degradation properties, *J. Environ. Chem. Eng.*, 9 (2021) 105390, doi: 10.1016/j.jece.2021.105390.
- [8] Z. Jemaat, M.E. Suárez-Ojeda, J. Pérez, J. Carrera, Simultaneous nitritation and p-nitrophenol removal using aerobic granular biomass in a continuous airlift reactor, *Bioresour. Technol.*, 150 (2013) 307–313.
- [9] J. Huang, C. Yan, K. Huang, Removal of p-nitrophenol by a water-compatible hyper-cross-linked resin functionalized with formaldehyde carbonyl groups and XAD-4 in aqueous solution: a comparative study, *J. Colloid Interface Sci.*, 332 (2009) 60–64.
- [10] A.A. Pradhan, P.R. Gogate, Degradation of p-nitrophenol using acoustic cavitation and Fenton chemistry, *J. Hazard. Mater.*, 173 (2010) 517–522.
- [11] X. Chen, M. Murugananthan, Y. Zhang, Degradation of p-nitrophenol by thermally activated persulfate in soil system, *Chem. Eng. J.*, 283 (2016) 1357–1365.
- [12] J. Cai, Y. Zhang, Enhanced degradation of bisphenol S by persulfate activated with sulfide-modified nanoscale zero-valent iron, *Environ. Sci. Pollut. Res. Int.*, 29 (2022) 8281–8293.
- [13] H. Li, L. Yang, L. He, Y. Ma, X. Yan, L. Wu, Z. Zhang, Kinetics and mechanisms of chloramphenicol degradation in aqueous solutions using heat-assisted nZVI activation of persulfate, *J. Mol. Liq.*, 313 (2020) 113511, doi: 10.1016/j.molliq.2020.113511.
- [14] H. Dong, K. Hou, W. Qiao, Y. Cheng, L. Zhang, B. Wang, L. Li, Y. Wang, Q. Ning, G. Zeng, Insights into enhanced removal of TCE utilizing sulfide-modified nanoscale zero-valent iron activated persulfate, *Chem. Eng. J.*, 359 (2019) 1046–1055.
- [15] C. Gao, S. Chen, X. Quan, H. Yu, Y. Zhang, Enhanced Fenton-like catalysis by iron-based metal organic frameworks for degradation of organic pollutants, *J. Catal.*, 356 (2017) 125–132.
- [16] B. Kaur, L. Kuntus, P. Tikker, E. Kattel, M. Trapido, N. Dulova, Photo-induced oxidation of ceftriaxone by persulfate in the presence of iron oxides, *Sci. Total Environ.*, 676 (2019) 165–175.
- [17] Z.-H. Diao, X.-R. Xu, H. Chen, D. Jiang, Y.-X. Yang, L.-J. Kong, Y.-X. Sun, Y.-X. Hu, Q.-W. Hao, L. Liu, Simultaneous removal of Cr(VI) and phenol by persulfate activated with bentonite-supported nanoscale zero-valent iron: reactivity and mechanism, *J. Hazard. Mater.*, 316 (2016) 186–193.
- [18] M. Gu, U. Farooq, S. Lu, X. Zhang, Z. Qiu, Q. Sui, Degradation of trichloroethylene in aqueous solution by rGO supported nZVI catalyst under several oxic environments, *J. Hazard. Mater.*, 349 (2018) 35–44.
- [19] V. Kecić, Đ. Kerkez, M. Prica, O. Lužanin, M. Bečelić-Tomin, D.T. Pilipović, B. Dalmacija, Optimization of azo printing dye removal with oak leaves-nZVI/H₂O₂ system using statistically designed experiment, *J. Cleaner Prod.*, 202 (2018) 65–80.
- [20] R. Deewan, D.Y. Yan, P. Khamdahsag, V. Tanboonchuy, Remediation of arsenic-contaminated water by green zero-valent iron nanoparticles, *Environ. Sci. Pollut. Res. Int.*, 30 (2023) 90352–90361.
- [21] P.M.M. Soares, D.C.A. Lima, R.M. Cardoso, M.L. Nascimento, A. Semedo, Western Iberian offshore wind resources: more or less in a global warming climate?, *Appl. Energy*, 203 (2017) 72–90.
- [22] Y. Tan, N. Zhao, Q. Song, H. Ling, Alkali synergistic sulfide-modified nZVI activation of persulfate for phenanthrene removal, *J. Environ. Chem. Eng.*, 11 (2023) 109923, doi: 10.1016/j.jece.2023.109923.
- [23] G. Gopal, H. Sankar, C. Natarajan, A. Mukherjee, Tetracycline removal using green synthesized bimetallic nZVI-Cu and bentonite supported green nZVI-Cu nanocomposite: a comparative study, *J. Environ. Manage.*, 254 (2020) 109812, doi: 10.1016/j.jenvman.2019.109812.
- [24] S. Zhang, T. Wang, X. Guo, S. Chen, L. Wang, Adsorption and reduction of trichloroethylene by sulfidated nanoscale zerovalent iron (S-nZVI) supported by Mg(OH)₂, *Environ. Sci. Pollut. Res. Int.*, 30 (2023) 14240–14252.
- [25] P. Singh, P. Pal, P. Mondal, G. Saravanan, P. Nagababu, S. Majumdar, N. Labhsetwar, S. Bhowmick, Kinetics and mechanism of arsenic removal using sulfide-modified nanoscale zerovalent iron, *Chem. Eng. J.*, 412 (2021) 128667, doi: 10.1016/j.cej.2021.128667.
- [26] M.P. Rayaroth, K.P. Prasanthkumar, Y.-G. Kang, C.-S. Lee, Y.-S. Chang, Degradation of carbamazepine by singlet oxygen from sulfidized nanoscale zero-valent iron – citric acid system, *Chem. Eng. J.*, 382 (2020) 122828, doi: 10.1016/j.cej.2019.122828.
- [27] M.P. Rayaroth, C.-S. Lee, U.K. Aravind, C.T. Aravindakumar, Y.-S. Chang, Oxidative degradation of benzoic acid using Fe⁰- and sulfidized Fe⁰-activated persulfate: a comparative study, *Chem. Eng. J.*, 315 (2017) 426–436.
- [28] W. Guo, Q. Zhao, J. Du, H. Wang, X. Li, N. Ren, Enhanced removal of sulfadiazine by sulfidated ZVI activated persulfate process: performance, mechanisms and degradation pathways, *Chem. Eng. J.*, 388 (2020) 124303, doi: 10.1016/j.cej.2020.124303.
- [29] M.P. Rayaroth, D. Oh, C.S. Lee, Y.G. Kang, Y.S. Chang, *In-situ* chemical oxidation of contaminated groundwater using a sulfidized nanoscale zerovalent iron-persulfate system: insights from a box-type study, *Chemosphere*, 257 (2020) 127117, doi: 10.1016/j.chemosphere.2020.127117.
- [30] C.-C. Lin, S.-T. Hsu, Performance of nZVI/H₂O₂ process in degrading polyvinyl alcohol in aqueous solutions, *Sep. Purif. Technol.*, 203 (2018) 111–116.
- [31] L. Albarano, M. Toscanesi, M. Trifuoggi, M. Guida, G. Lofrano, G. Libralato, *In-situ* microcosm remediation of polyaromatic hydrocarbons: influence and effectiveness of nano-zero valent

- iron and activated carbon, *Environ. Sci. Pollut. Res. Int.*, 30 (2023) 3235–3251.
- [32] X. Chen, G. Fan, H. Li, Y. Li, R. Zhang, Y. Huang, X. Xu, Nanoscale zero-valent iron particles supported on sludge-based biochar for the removal of chromium(VI) from aqueous system, *Environ. Sci. Pollut. Res.*, 29 (2022) 3853–3863.
- [33] W. Zhang, L. Qian, D. Ouyang, Y. Chen, L. Han, M. Chen, Effective removal of Cr(VI) by attapulgite-supported nanoscale zero-valent iron from aqueous solution: enhanced adsorption and crystallization, *Chemosphere*, 221 (2019) 683–692.
- [34] X. Chen, J. Cui, X. Xu, B. Sun, L. Zhang, W. Dong, C. Chen, D. Sun, Bacterial cellulose/attapulgite magnetic composites as an efficient adsorbent for heavy metal ions and dye treatment, *Carbohydr. Polym.*, 229 (2020) 115512, doi: 10.1016/j.carbpol.2019.115512.
- [35] A. Maleki, Z. Hajizadeh, V. Sharifi, Z. Emdadi, A green, porous and eco-friendly magnetic geopolymer adsorbent for heavy metals removal from aqueous solutions, *J. Cleaner Prod.*, 215 (2019) 1233–1245.
- [36] L. Zhao, K. Shen, B. Li, Y. Zhang, S. Zhang, Y. Hong, J. Zhang, Z. Li, Exploration of novel high-temperature heavy metals adsorbent for sludge incineration process: experiments and theoretical calculations, *J. Environ. Chem. Eng.*, 10 (2022) 107755, doi: 10.1016/j.jece.2022.107755.
- [37] M. Chen, H. Xu, Y. Zhang, X. Zhao, Y. Chen, X. Kong, Effective removal of heavy metal ions by attapulgite supported sulfidized nanoscale zerovalent iron from aqueous solution, *Colloids Surf., A*, 640 (2022) 128192, doi: 10.1016/j.colsurfa.2021.128192.
- [38] H. Dong, B. Wang, L. Li, Y. Wang, Q. Ning, R. Tian, R. Li, J. Chen, Q. Xie, Activation of persulfate and hydrogen peroxide by using sulfide-modified nanoscale zero-valent iron for oxidative degradation of sulfamethazine: a comparative study, *Sep. Purif. Technol.*, 218 (2019) 113–119.
- [39] S.K. Mondal, A.K. Saha, A. Sinha, Removal of ciprofloxacin using modified advanced oxidation processes: kinetics, pathways and process optimization, *J. Cleaner Prod.*, 171 (2018) 1203–1214.
- [40] L. Wang, J. Yang, Y. Li, J. Lv, J. Zou, Removal of chlorpheniramine in a nanoscale zero-valent iron induced heterogeneous Fenton system: influencing factors and degradation intermediates, *Chem. Eng. J.*, 284 (2016) 1058–1067.
- [41] A. Iqbal, Y. Tian, X. Wang, D. Gong, Y. Guo, K. Iqbal, Z. Wang, W. Liu, W. Qin, Carbon dots prepared by solid state method via citric acid and 1,10-phenanthroline for selective and sensing detection of Fe²⁺ and Fe³⁺, *Sens. Actuators, B*, 237 (2016) 408–415.
- [42] Y. Yao, N. Mi, C. He, H. He, Y. Zhang, Y. Zhang, L. Yin, J. Li, S. Yang, S. Li, L. Ni, Humic acid modified nano-ferrous sulfide enhances the removal efficiency of Cr(VI), *Sep. Purif. Technol.*, 240 (2020) 116623, doi: 10.1016/j.seppur.2020.116623.
- [43] Q. Wang, J. Wen, X. Hu, L. Xing, C. Yan, Immobilization of Cr(VI) contaminated soil using green-tea impregnated attapulgite, *J. Cleaner Prod.*, 278 (2021) 123967, doi: 10.1016/j.jclepro.2020.123967.
- [44] D. Lv, X. Zhou, J. Zhou, Y. Liu, Y. Li, K. Yang, Z. Lou, S.A. Baig, D. Wu, X. Xu, Design and characterization of sulfide-modified nanoscale zerovalent iron for cadmium(II) removal from aqueous solutions, *Appl. Surf. Sci.*, 442 (2018) 114–123.
- [45] W. Zhang, H. Gao, J. He, P. Yang, D. Wang, T. Ma, H. Xia, X. Xu, Removal of norfloxacin using coupled synthesized nanoscale zero-valent iron (nZVI) with H₂O₂ system: optimization of operating conditions and degradation pathway, *Sep. Purif. Technol.*, 172 (2017) 158–167.
- [46] F. Zhu, Y. Wu, Y. Liang, H. Li, W. Liang, Degradation mechanism of norfloxacin in water using persulfate activated by BC@nZVI/Ni, *Chem. Eng. J.*, 389 (2020) 124276, doi: 10.1016/j.cej.2020.124276.
- [47] A. Shan, A. Idrees, W.Q. Zaman, Z. Abbas, M. Ali, M.S.U. Rehman, S. Hussain, M. Danish, X. Gu, S. Lyu, Synthesis of nZVI-Ni@BC composite as a stable catalyst to activate persulfate: trichloroethylene degradation and insight mechanism, *J. Environ. Chem. Eng.*, 9 (2021) 104808, doi: 10.1016/j.jece.2020.104808.
- [48] H. Liu, T. Chen, Q. Xie, X. Zou, C. Chen, R.L. Frost, The functionalization of limonite to prepare NZVI and its application in decomposition of p-nitrophenol, *J. Nanopart. Res.*, 17 (2015) 374, doi: 10.1007/s11051-015-3171-6.
- [49] T.-L. Ren, X.-W. Ma, X.-Q. Wu, L. Yuan, Y.-L. Lai, Z.-H. Tong, Degradation of imidazolium ionic liquids in a thermally activated persulfate system, *Chem. Eng. J.*, 412 (2021) 128624, doi: 10.1016/j.cej.2021.128624.
- [50] Q. Jiang, Y. Zhang, S. Jiang, Y. Wang, H. Li, W. Han, J. Qu, L. Wang, Y. Hu, Graphene-like carbon sheet-supported nZVI for efficient atrazine oxidation degradation by persulfate activation, *Chem. Eng. J.*, 403 (2021) 126309, doi: 10.1016/j.cej.2020.126309.
- [51] Q. Mao, Y. Zhou, Y. Yang, J. Zhang, L. Liang, H. Wang, S. Luo, L. Luo, P. Jeyakumar, Y.S. Ok, M. Rizwan, Experimental and theoretical aspects of biochar-supported nanoscale zero-valent iron activating H₂O₂ for ciprofloxacin removal from aqueous solution, *J. Hazard. Mater.*, 380 (2019) 120848, doi: 10.1016/j.jhazmat.2019.120848.
- [52] A.R. Rahmani, M. Salari, A. Shabanloo, N. Shabanloo, S. Bajalan, Y. Vaziri, Sono-catalytic activation of persulfate by nZVI-reduced graphene oxide for degradation of nonylphenol in aqueous solution: process optimization, synergistic effect and degradation pathway, *J. Environ. Chem. Eng.*, 8 (2020) 104202, doi: 10.1016/j.jece.2020.104202.
- [53] J. Du, Y. Wang, Faheem, T. Xu, H. Zheng, J. Bao, Synergistic degradation of PNP via coupling H₂O₂ with persulfate catalyzed by nano zero valent iron, *RSC Adv.*, 9 (2019) 20323–20331.
- [54] Y. Du, M. Dai, I. Naz, X. Hao, X. Wei, R. Rong, C. Peng, I. Ali, Carbothermal reduction synthesis of zero-valent iron and its application as a persulfate activator for ciprofloxacin degradation, *Sep. Purif. Technol.*, 275 (2021) 119201, doi: 10.1016/j.seppur.2021.119201.
- [55] P. Xu, L. Wang, X. Liu, S. Xie, Z. Yang, P. Zhu, Ascorbic acid enhanced the zero-valent iron/peroxymonosulfate oxidation: simultaneous chelating and reducing, *Sep. Purif. Technol.*, 298 (2022) 121599, doi: 10.1016/j.seppur.2022.121599.
- [56] W. Xu, X. Hu, Y. Lou, X. Jiang, K. Shi, Y. Tong, X. Xu, C. Shen, B. Hu, L. Lou, Effects of environmental factors on the removal of heavy metals by sulfide-modified nanoscale zerovalent iron, *Environ. Res.*, 187 (2020) 109662, doi: 10.1016/j.envres.2020.109662.
- [57] X. Yang, S. Yu, M. Wang, Q. Liu, X. Jing, X. Cai, One-pot preparations of cyclodextrin polymer-entrapped nano zero-valent iron for the removal of p-nitrophenol in water, *Chem. Eng. J.*, 431 (2022) 133370, doi: 10.1016/j.cej.2021.133370.
- [58] M. Vogel, A. Georgi, F.-D. Kopinke, K. Mackenzie, Sulfidation of ZVI/AC composite leads to highly corrosion-resistant nanoremediation particles with extended life-time, *Sci. Total Environ.*, 665 (2019) 235–245.
- [59] A.N. Garcia, Y. Zhang, S. Ghoshal, F. He, D.M. O'Carroll, Recent advances in sulfidated zerovalent iron for contaminant transformation, *Environ. Sci. Technol.*, 55 (2021) 8464–8483.
- [60] L. Tang, J. Tang, G. Zeng, G. Yang, X. Xie, Y. Zhou, Y. Pang, Y. Fang, J. Wang, W. Xiong, Rapid reductive degradation of aqueous p-nitrophenol using nanoscale zero-valent iron particles immobilized on mesoporous silica with enhanced antioxidation effect, *Appl. Surf. Sci.*, 333 (2015) 220–228.
- [61] B. Lai, Z. Chen, Y. Zhou, P. Yang, J. Wang, Z. Chen, Removal of high concentration p-nitrophenol in aqueous solution by zero valent iron with ultrasonic irradiation (US-ZVI), *J. Hazard. Mater.*, 250–251 (2013) 220–228.

Supplementary information

Table S1
Basic chemical properties of PNP

Name	Molecular weight (g·mol ⁻¹)	λ_{\max}	Structure
p-nitrophenol	139.11	317nm	

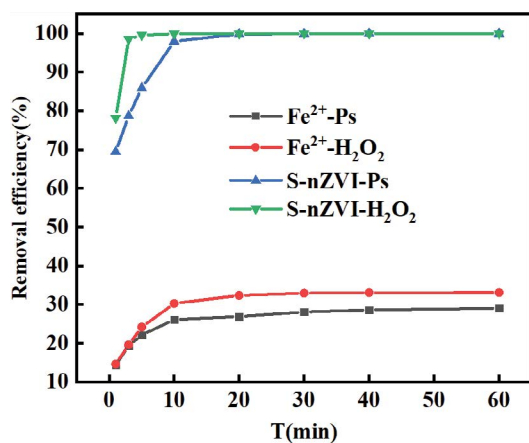
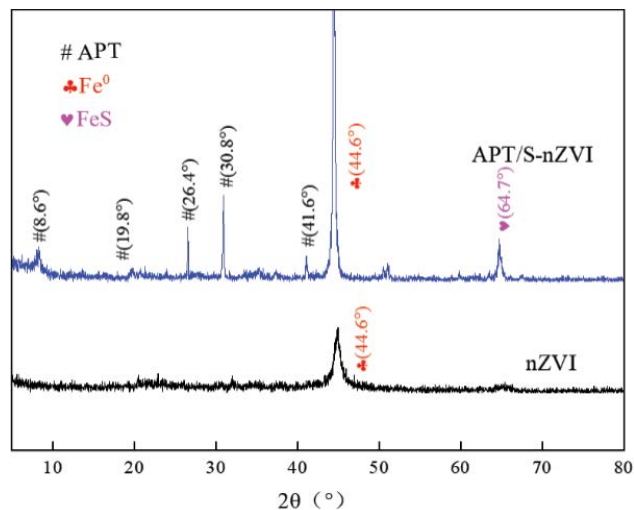
Fig. S1. Removal efficiency of PNP in homogeneous oxidation systems (PNP = 50 mg·L⁻¹, Fe²⁺ = 5mM, S/Fe = 0.3, initial pH = 3.0, Ps = 6 mM, H₂O₂ = 6 mM).

Fig. S2. X-ray diffraction characterization of nZVI and APT/S-nZVI.

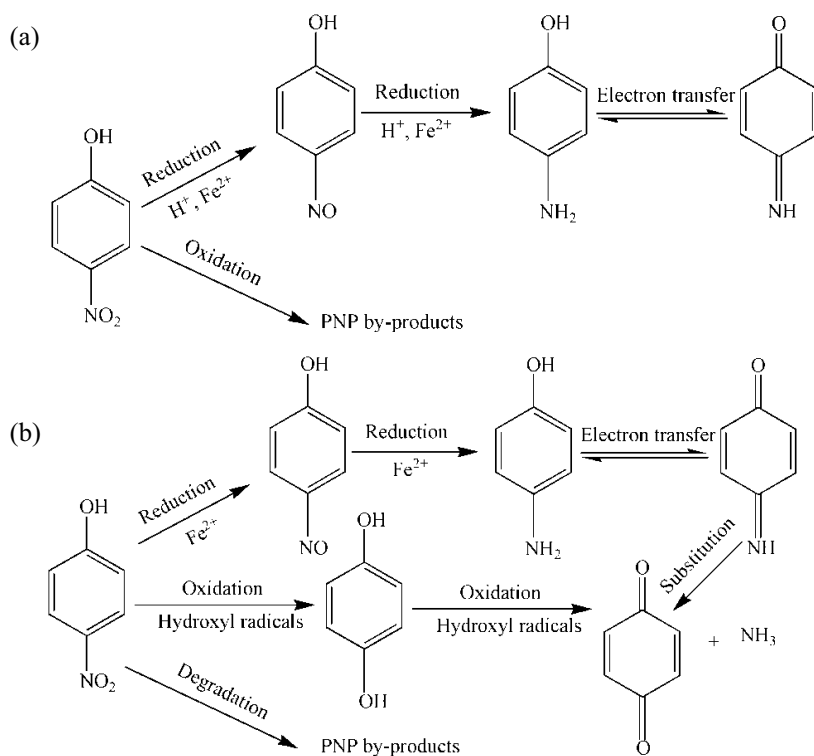
Fig. S3. Possible degradation pathway of PNP by APT/S-nZVI activation of Ps (a) and H₂O₂ (b).

Table S2
Degradation products of p-nitrophenol in APT/S-nZVI/Ps system

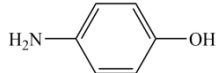
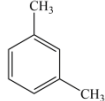
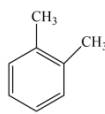
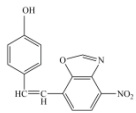
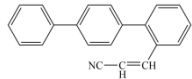
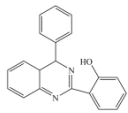
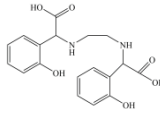
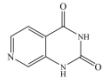
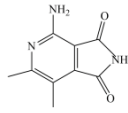
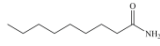
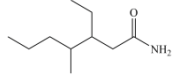
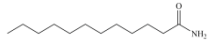
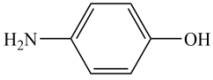
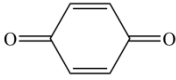
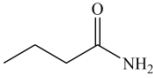
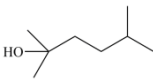
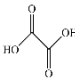
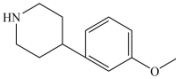
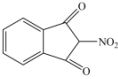
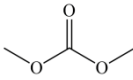
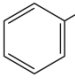

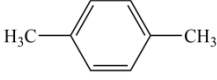

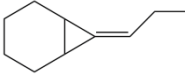
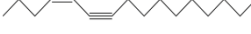
No.	Name	Formula	Chemical constitution
1	p-Aminophenol	C_6H_7ON	
2	o-Xylene	C_8H_{10}	
3	1,3-Dimethyl-benzene	C_8H_{10}	
4	4-[2-(5-nitro-2-benzoxazolyl)ethenyl]-phenol	$C_{15}H_{10}O_4N_2$	
5	1-phenyl-4-(2-cyano-2-phenylethenyl)-benzene	$C_{21}H_{15}N$	
6	2-[4-(2-hydroxyethylamino)-2-quinazoliny]-phenol	$C_{20}H_{14}N_2O$	
7	N,N'-Ethylenebis(2-[2-hydroxyphenyl]glycine)	$C_{16}H_{18}O_6N_2$	
8	Pyrido[3,4-d]pyrimidine-2,4(1H,3H)-dione	$C_7H_5O_2N_2$	
9	1H-Pyrrolo[3,4-c]pyridine-1,3,(2H)-dione	$C_9H_{11}O_2N_3$	
10	Nonanamide	$C_9H_{19}ON$	
11	4-Ethyl-5-methyl-heptanamide	$C_{10}H_{21}ON$	
12	Tetradecanamide	$C_{14}H_{29}ON$	

Table S3
Degradation products of p-nitrophenol in APT/S-nZVI/H₂O₂ system

No.	Name	Formula	Chemical constitution
1	p-Aminophenol	C ₆ H ₇ ON	
2	p-benzoquinone	C ₆ H ₄ O ₂	
3	Butanamide	C ₄ H ₉ ON	
4	2,5-dimethyl-2-Hexanol	C ₈ H ₁₈ O	
5	Ketene	C ₂ H ₂ O	O=C=CH ₂
6	Ethanedioic acid	C ₂ H ₂ O ₄	
7	N-[3-methoxyphenyl]-piperidine	C ₁₁ H ₁₇ ON	
8	2-Nitro-1,3-indanedione	C ₉ H ₅ O ₄ N	
9	Carbamic acid	C ₃ H ₆ O ₃	
10	Ethylbenzene	C ₈ H ₁₀	
11	2,4-Octadiyne	C ₈ H ₁₄	
12	p-Xylene	C ₈ H ₁₀	
13	1,6-Heptadiyne	C ₇ H ₈	
14	7-Propylidene-bicyclo[4.1.0]heptane	C ₁₀ H ₁₆	
15	(Z)-4-Hexadecen-6-yne	C ₁₆ H ₂₈	
16	1-Methyl-2-methylene-cycloheptanol	C ₉ H ₁₅ O	